Cutaneous haptic feedback to ensure the stability of robotic teleoperation systems

Article *in* The International Journal of Robotics Research · October 2015

DOI: 10.1177/0278364915603135

CITATIONS
62

READS
271

5 authors, including:

Claudio Pacchierotti
French National Centre for Scientific Research
92 PUBLICATIONS **1,487** CITATIONS
SEE PROFILE

Leonardo Meli
Università degli Studi di Siena
27 PUBLICATIONS **430** CITATIONS
SEE PROFILE

Francesco Chinello
Aarhus University
32 PUBLICATIONS **653** CITATIONS
SEE PROFILE

Monica Malvezzi
Università degli Studi di Siena
127 PUBLICATIONS **2,151** CITATIONS
SEE PROFILE

Cutaneous haptic feedback to ensure the stability of robotic teleoperation systems

C. Pacchierotti, L. Meli, F. Chinello, M. Malvezzi, and D. Prattichizzo

***Abstract*—Cutaneous haptic feedback can be used to enhance the performance of robotic teleoperation systems while guaranteeing their safety. Delivering ungrounded cutaneous cues to the human operator conveys in fact information about the forces exerted at the slave side and does not affect the stability of the control loop. In this work we analyze the feasibility, effectiveness, and implications of providing solely cutaneous feedback in robotic teleoperation. We carried out two peg-in-hole experiments, both in a virtual environment and in a real (teleoperated) environment. Two novel 3-degree-of-freedom fingertip cutaneous displays deliver a suitable amount of cutaneous feedback at the thumb and index fingers. Results assessed the feasibility and effectiveness of the proposed approach. Cutaneous feedback was outperformed by full haptic feedback provided by grounded haptic interfaces, but it outperformed conditions providing no force feedback at all. Moreover, cutaneous feedback always kept the system stable, even in the presence of destabilizing factors such as communication delays and hard contacts.**

I. Introduction

Teleoperation systems are employed to sense and mechanically manipulate objects at a distance by virtually relocating the operator at a place other than his or her true location (Sheridan 1995, Hirche et al. 2007). They are composed of a slave system, which interacts with the remote environment, and a master system, operated by a human. The slave system includes sensors to perceive the environment, actuators to physically interact with it, and network channels to communicate with the master side. The human operator should then receive enough information about the slave system and the remote environment to feel physically present at the remote site. This condition is commonly referred to as *telepresence* (Sheridan 1989, 1992).

Achieving a good illusion of telepresence is a matter of technology. If the slave system transmits sufficient information back to the operator, displayed in a sufficiently natural way, the illusion of telepresence can be compelling (Sheridan 1992, Hirche et al. 2007). This can be achieved through different types of feedback information, that flow from the remote scenario to the human operator. One piece of this flow is haptic feedback, that conveys information about the forces exerted at the slave side of the system. Haptic feedback is provided to the human operator through cutaneous and kinesthetic stimuli. Cutaneous stimuli are detected by mechanoreceptors in the skin, enabling humans to recognize the local properties of objects such as shape, edges, and texture. Cutaneous perception for exploration and manipulation principally relies on measures of the location, intensity, direction, and timing of contact forces on the fingertips (Birznieks et al. 2001, Johnson 2001). On the other hand, kinesthesia provides humans with information about the position and velocity of neighboring body parts, as well as the applied force and torque, mainly by means of receptors in the muscles and joints (Hayward et al. 2004, Edin & Johansson 1995).

Visual feedback is already available in teleoperation systems (e.g., the Intuitive Surgical da Vinci robot), but current systems have very limited haptic feedback. This omission is mainly due to the negative effect that haptic feedback has on the stability of the control loop (see Fig. 1a). Time-varying destabilizing factors, such as hard contacts, relaxed user grasps, stiff control settings, and communication delays, can in fact significantly affect the stability and transparency of teleoperation systems, reducing their applicability and effectiveness (Lawrence 1993). Nonetheless, haptic feedback has been proved to play an important role in enhancing the performance of teleoperation systems in terms of task completion time (Massimino & Sheridan 1994, Moody et al. 2002, Pacchierotti et al. 2012a), accuracy (Moody et al. 2002, Prattichizzo et al. 2012), peak and mean exerted force (Hannaford 1987, Wagner et al. 2002, Pacchierotti et al. 2012a).

Therefore, guaranteeing the stability and transparency of teleoperation systems with haptic feedback has always been a great challenge. To this aim, researchers have proposed a great variety of transparency- and stability-optimized bilateral controllers (Salcudean 1998, Hokayem & Spong 2006), and it has always been difficult to find a good trade-off between these two objectives. In this respect, passivity (van der Schaft 2000) has been exploited as the main tool for providing a sufficient condition for stable teleoperation in several controller design approaches, such as the Scattering Algorithm (Niemeyer & Slotine 2004), Time Domain Passivity Control (Ryu et al. 2004), Energy Bounding Algorithm (Kim & Ryu 2010), and Passive Set Position Modulation (Lee & Huang 2010).

Another approach to stability in teleoperation consists of avoiding the usage of actuators on the master side and then substituting haptic feedback with stimuli of another sensory modality, such as vibrotactile (Schoonmaker & Cao 2006), auditory, and/or visual feedback (Kitagawa et al. 2005). This technique is commonly referred to as *sensory substitution* (Massimino 1995). Because no haptic force is provided to the human operator, sensory substitution makes teleoperation systems intrinsically stable (Prattichizzo et al. 2012, 2010). However, although the stability of the system is guaranteed, the provided stimuli differ substantially from the ones being sub-

L. Meli, F. Chinello, M. Malvezzi and D. Prattichizzo are with the Department of Information Engineering and Mathematics, University of Siena, via Roma 56, 53100 Siena, Italy.
C. Pacchierotti, L. Meli, and D. Prattichizzo are with the Department of Advanced Robotics, Istituto Italiano di Tecnologia, via Morego 30, 16163 Genova, Italy.
Corresponding author; e-mail: pacchierotti@dii.unisi.it

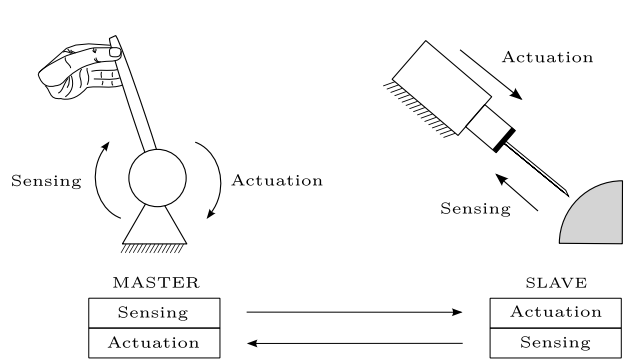

(a) Common approach for teleoperation systems. The force fed back to the user is applied directly on the end-effector of the master device, which is also in charge of steering the slave robot. A control action is needed to avoid instability.

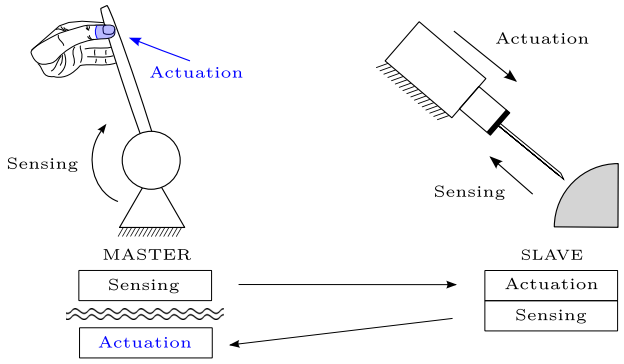

(b) Teleoperation system employing cutaneous feedback only. Force feedback is applied to the fingertips of the operator and the loop is intrinsically stable.

Fig. 1. Common approach for teleoperation vs. our cutaneous-only sensory subtraction technique. The loss of realism due to solely providing cutaneous force may be in some scenarios a price worth paying to gain a great improvement in the safety of the system.

stituted (e.g., a beep sound instead of force feedback). Therefore, sensory substitution often shows performance inferior to that achieved with unaltered force feedback (Prattichizzo et al. 2012).

Similarly to sensory substitution, Prattichizzo et al. (2012) presented a feedback technique that substitutes full haptic feedback, consisting of cutaneous and kinesthetic components (Birznieks et al. 2001, Hayward et al. 2004, Pacchierotti et al. 2014), with cutaneous feedback only. They showed that cutaneous feedback provided by a moving platform is more effective than sensory substitution via visual feedback in a teleoperated needle insertion task. Moreover, they showed that cutaneous feedback did not affect the stability of the teleoperation loop, even in the presence of destabilizing factors such as time delays and hard contacts. Similar to the moving platform used by Prattichizzo et al. (2012), pneumatic balloon-based systems are another popular approach used by researchers to relay cutaneous feedback via contact force in teleoperation (King et al. 2009b, Li et al. 2013).

Further possible techniques provide cutaneous stimuli via tactile vibrations (Kontarinis & Howe 1995, McMahan et al. 2011, Pacchierotti et al. 2015) and skin stretch (Provancher & Sylvester 2009, Webster III et al. 2005, Kurita et al. 2011, Quek et al. 2015). The system created by McMahan et al. (2011) for the Intuitive da Vinci robot, for example, enables surgeons to feel the slave instrument vibrations in real time without destabilizing the teleoperation loop. More recently, Quek et al. (2015) designed a 3-degree-of-freedom (3-DoF) skin stretch cutaneous device to substitute full haptic feedback with skin stretch cutaneous stimuli in teleoperation. Providing skin stretch feedback together with kinesthetic feedback led to higher performance than providing kinesthetic feedback alone. Prattichizzo et al. (2012) call this overall cutaneous-only feedback approach *sensory subtraction*, in contrast to *sensory substitution*, as it subtracts the destabilizing kinesthetic part of the full haptic interaction to leave only cutaneous cues.

In this work we discuss the feasibility and effectiveness of the sensory subtraction approach in teleoperation. Instead of rendering full haptic feedback via grounded haptic interfaces, we propose to provide the human operator with cutaneous stimuli only. We expect this kind of feedback to make the teleoperation system stable, since the cutaneous force applied does not affect the position of the master device (see Fig. 1b). Furthermore, as in (Prattichizzo et al. 2012), we expect the human operator to perform the given tasks in an equally intuitive way, since cutaneous stimuli provide the user with a rich and co-located perception of the contact force. We analyze the implications and outcomes of such an approach for two peg-in-hole experiments, in virtual and real scenarios, employing two novel 3-DoF fingertip cutaneous devices. Each device exerts cutaneous stimuli at the fingertip by applying forces to the vertices of a rigid platform. With respect to the work presented by Prattichizzo et al. (2012), we extended the evaluation and discussion to a multi-DoF and more challenging scenario, we carried out one experiment in real environment, and we employed a novel set of cutaneous devices that show better dynamic performance and higher peak forces.

The rest of the paper is organized as follows. The cutaneous device is presented in Sec. II, together with its kinematics and statics analysis. The experiment in a virtual environment is presented in Sec. III, while the experiment in a real (teleoperated) environment is presented in Sec. IV. Finally, Sec. V addresses concluding remarks and perspectives of the work.

II. A 3-DoF Fingertip Cutaneous Device

To demonstrate the feasibility and performance of the sensory subtraction approach, we designed a novel 3-DoF cutaneous haptic device. It is able to provide cutaneous stimuli at the fingertip, and it can be easily attached to the end-effector of commercial haptic interfaces. Fig. 2a sketches the main idea, while a prototype of the device is shown in Fig. 2b[1]. It is composed of a static body (A, C-E in Fig. 2a) that houses three servo motors (B) above the user's fingernail and a mobile

[1]A video of the proposed device can be downloaded at http://goo.gl/C8KUWZ

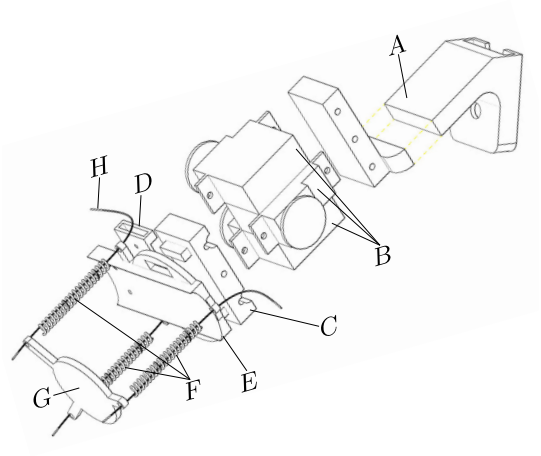

(a)

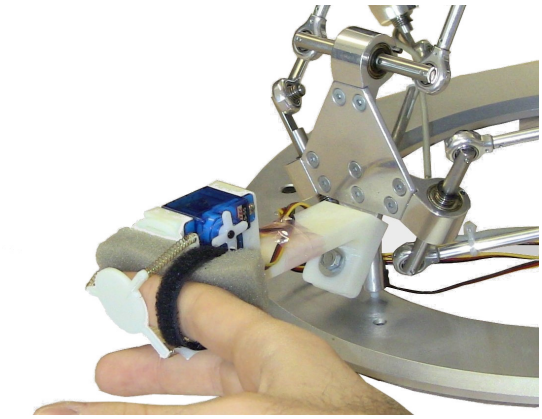

(b)

Fig. 2. The 3-DoF fingertip cutaneous device. It is composed of a static body (A, C-E) that houses three servo motors (B) and a mobile platform (G) that applies the requested stimuli to the fingertip. Three cables (H) and springs (F) connect the two platforms. By controlling the cable lengths, the motors can orient and translate the mobile platform in three-dimensional space. The device fastens to the finger with a fabric strap fixed to part D. The device can be easily attached to the end-effector of different commercial haptic devices.

platform (G) that applies the requested stimuli to the fingertip. Three cables (H) connect the two platforms, and springs (F) around the cables keep the mobile platform in a reference configuration, away from the fingertip, when not actuated. By controlling the cables length, the motors can orient and translate the mobile platform in three-dimensional space. The device fastens to the finger with a fabric strap fixed to part D.

The actuators we used are HS-55 MicroLite (Hitec RCD Korea, KR) servo motors. They are able to exert up to 120 N·mm torque. The mechanical support is realized using a special type of acrylonitrile butadiene styrene, called ABS*Plus* (Stratasys Inc., USA). The total weight of the device, including actuators, springs, wires, and mechanical support, is 45 g. The force applied by the device to the user's finger pad is balanced by a reaction force supported by the body of the device (E). This structure has a larger contact surface with respect to the mobile platform (G), so that the local pressure is lower and the contact is thus mainly perceived on the finger pad and not on the nail side of the finger (Prattichizzo et al. 2013). More details on the device's technical specifications are shown in Table I. This 3-DoF cutaneous device has been preliminary presented in (Pacchierotti et al. 2012a).

General	
Actuators	HS-55 servo motor (max current 1A)
Power Supply	external adapter 6V 1A
Controller	Atmega 328 on an Arduino Nano board
Motor bandwidth	100 Hz
Platform	
Max normal force	20 N
Max tangential force	8 N
Max roll angle	25 deg
Max pitch angle	25 deg
Max speed	21 mm/s

TABLE I
TECHNICAL SPECIFICATIONS OF THE FINGERTIP CUTANEOUS DEVICE.

A. Device model and control

This section summarizes the device working principles and analyzes the range of forces the device can apply. For the applicable forces, two types of constraints are considered: the first one is due to the friction between the finger pad and the platform, while the second one is due to the device mechanical structure and actuation system. To define the subspace of forces the device can generate, we assume that the system, composed of the device and the fingertip, is in static equilibrium conditions. We then neglect platform displacement due to force variations. In fact, in order to take into account for the effect of this displacement, we would need to know more about the fingertip compliance features, that are not easy to evaluate and are subject-related (Wiertlewski & Hayward 2012).

Device geometry and forces. Similarly to the wearable device presented by Prattichizzo et al. (2013), our cutaneous system can be modeled as a 3-DoF parallel mechanism, where the static body is fixed to the nail side of the finger and the mobile platform is in contact with the finger pulp. The platform is actuated by controlling the length and tension of three cables connected to its vertices. When no torques are applied to the motors, three springs maintain the platform in a reference configuration, constraining its motion in the normal and tangential directions. However, in the following quasi-static analysis, for the sake of simplicity, we neglect the springs stiffness in the lateral direction. The mechanical model of this device differs from the one described by Prattichizzo et al. (2013), since, in our case, cable directions are not influenced by the finger geometry and curvature. Thanks to a larger mobile platform, cables never touch the finger and, therefore, no problems due to the friction between cables and skin arise.

In Fig. 3a and 3b, B_1, B_2, and B_3 indicate the points, on the mobile platform, where the cables, linking the mobile platform to the three motors, pass. $S_1 = \langle O_1, x, y, z \rangle$ is a reference frame on the mobile platform, whose origin O_1 is placed at the platform's geometric center and whose z axis is orthogonal to the plane defined by B_i, pointing towards the fingertip. A_1, A_2, and A_3 indicate the points, on the static body of the device, where the cables pass, and $S_0 = \langle O_0, x_0, y_0, z_0 \rangle$

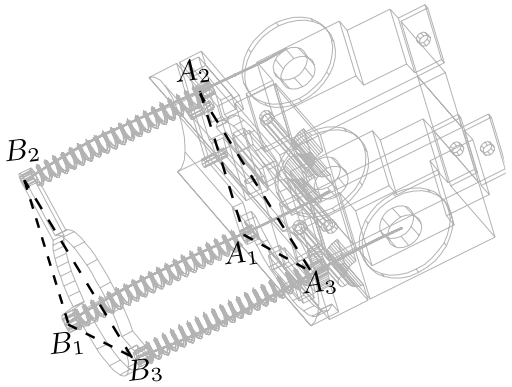

(a) Device kinematic scheme.

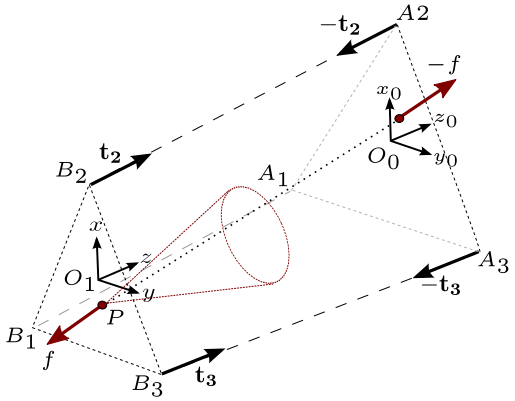

(b) Forces acting on the device.

Fig. 3. The 3-DoF cutaneous device model. In (a), A_i and B_i are the points where the cables link the static and mobile parts of the device, respectively. In (b), force $\mathbf{f}$ is applied by the fingertip to the device at point P. Its direction has to be inside the friction cone (in red) in order to fulfil our friction constraint. On the other hand, $\mathbf{t_i}$ represent the forces applied by the actuators to the mobile platform.

is a reference frame on that body, whose origin is located at O_0, and whose z_0 axis is orthogonal to the plane defined by A_i.

Wrench $\mathbf{w_p} = [\mathbf{f}^{\mathrm{T}}, \mathbf{m}^{\mathrm{T}}]^{\mathrm{T}}$, applied by the fingertip on the platform and expressed with respect to point P, is balanced by the forces $\mathbf{t_1}$, $\mathbf{t_2}$, and $\mathbf{t_3}$ applied by the three cables (see Fig. 3b). Point P can be defined as the intersection between the central axis of the stress distribution and the plane defined by points B_i. Even though the contact between the fingertip and the mobile platform is approximately at the center of the mobile platform, for the sake of generality, we consider $P \neq O_1$.

Contact and friction. The ratio between the tangential and the normal component of the contact force $\mathbf{f}$, in classical friction models, is limited by the friction coefficient μ, that depends on the surface material and conditions. This constraint has a meaningful graphical interpretation, that is shown in Fig. 3b: the direction of the contact force $\mathbf{f}$ has to lie within a cone, (i) whose axis is the normal direction to the contact surface at the (theoretical) contact point, (ii) whose vertex is point P itself, and (iii) has a vertex angle of $\varphi = \arctan \mu$. This cone is usually referred to as a *friction cone* (Salisbury & Tarr 1997).

Device equilibrium. The directions of forces $\mathbf{t_1}$, $\mathbf{t_2}$, and $\mathbf{t_3}$ are defined, respectively, by the unitary vectors $\mathbf{s_1}$, $\mathbf{s_2}$, and $\mathbf{s_3}$, that go from the mobile platform to the static body. These forces can be thus expressed as the sum of two components: the first one is the force applied by the i-th actuator and its module depends on the motor torque, while the second one is the contribution generated by the spring and its module depends on the spring stiffness and deformation. Forces $\mathbf{t_i}$, with $i = 1, \ldots, 3$ can be then expressed as

$$\mathbf{t_i} = t_i \mathbf{s_i}, \quad t_i = \left(\frac{\eta_i}{r_i} - k_i \left(|d_i| - |d_{i,o}| \right) \right), \tag{1}$$

where η_i is the torque of the i-th motor, r_i is the i-th motor pulley radius ($r_i = 8$ mm in our case), k_i is the spring stiffness ($k_i = 0.7$ N/mm in our case), $|d_i|$ the actual cable length, and $|d_{i,0}|$ the nominal spring length ($|d_{i,0}| = 20$ mm in our case).

Beside the friction cone, which substantially depends on the properties of the contact surface, the structure of the device itself imposes additional constraints on the direction of the contact force. For any given set of forces $\mathbf{t_1}$, $\mathbf{t_2}$, and $\mathbf{t_3}$, for any relative configuration between the parts of the device, and for any given contact point, the force and momentum equilibrium equations lead to

$$-\mathbf{w_p} = \begin{bmatrix} \mathbf{s_1} & \mathbf{s_2} & \mathbf{s_3} \\ \mathbf{S(b_1)} & \mathbf{S(b_2)} & \mathbf{S(b_3)} \end{bmatrix} \mathbf{t} = \mathbf{A}\,\mathbf{t}, \tag{2}$$

where $\mathbf{t} = [t_1, \ t_2, \ t_3]^{\mathrm{T}}$, $\mathbf{b_i}$ are three vectors defined as $\mathbf{b_i} = (B_i - P)$, and $S(\mathbf{b_i})$ denotes the skew matrix associated with the vectors $\mathbf{b_i}$. For any given configuration, the possible wrenches that can be generated are therefore those belonging to the column space of matrix $\mathbf{A}$. However, it is not possible to define an inverse relationship between wrenches and forces. In other terms, since the device is underactuated, it is not possible to arbitrarily set the wrench $\mathbf{w_p}$ and evaluate $\mathbf{t_i}$ from it.

Maximum force inclination. Assuming $t_i \geq 0$ and considering the structure of the device for any contact point and any device configuration, it is easy to assess from eq. (2) that the maximum inclination ϕ_{max} of force $\mathbf{f}$, with respect to the normal direction identified by the z axis, is given by

$$\phi_{max} = \max_{i=1,2,3} \left(\arcsin |\mathbf{s_i} \times \mathbf{k}| \right), \tag{3}$$

where $\mathbf{k}$ denotes the unit vector parallel to the z axis. This is another constraint for the contact force the device can apply to the fingertip, and it only depends on the geometry and structure of the device. Also this second constraint has a graphical interpretation: the force $\mathbf{f}$ has to stay inside a pyramidal surface with a triangular basis, whose vertex is in P and whose lateral edges are defined by the directions parallel to $\mathbf{s_1}$, $\mathbf{s_2}$, and $\mathbf{s_3}$. The range of applicable force directions thus depends on the inclination of the $\mathbf{s_i}$ vectors with respect to the platform. In order to be able to apply a wider range of forces, i.e., higher tangential forces with respect to the normal ones, it is necessary to increase these inclinations. For example, we could increase the size of the static body, the one placed on the nail side of the finger, and/or shape the device to reduce the distance between points A_i and B_i in the z direction.

Design for stability. Unlike other interfaces designed to apply solely shear stresses (Solazzi et al. 2011, Quek et al.

2013), our cutaneous device can provide only forces with a maximum inclination ϕ_{max}. This means that a component of the force normal to the fingertip surface will always be present and clearly perceivable. Although this limits the actuation capabilities of our device, it also suggests a very interesting mechanical property. A force applied by the mobile platform to the fingertip will be always compensated by a reaction force supported by the static body of the device (called E in Fig. 2a). This reaction force is balanced by the contact with the finger nail and by the joints of the grounded haptic device (see Fig. 2b). The ratio between these two force components depends on the fingertip and Omega compliances, both evaluated with respect to the point in which the cutaneous device is located. We assume that the part of the reaction force applied to the Omega is much smaller with respect to the other forces involved. In the hypothesis that this force component can be neglected, as introduced in Sec. I, this type of cutaneous feedback does not affect the stability of the teleoperation system in which it is employed, since the force is provided *only* at the fingertip level and does not influence the position of the master end-effector. The validity of this assumption is confirmed by the experiments described in Secs. III and IV.

Contact stiffness. The platform deforms the fingertip by applying a wrench $-\mathbf{w_p}$. Any displacement of the platform $\boldsymbol{\xi} = [p_x\ p_y\ p_z\ \alpha\ \beta\ \gamma]^{\mathrm{T}}$ when in contact with the finger, leads to a contact stress distribution on the finger pad. The resultant force and moment of the normal and tangential stress distributions, arising at the contact patch, balance the external wrench $-\mathbf{w_p}$. Fingertip deformation and applied wrench can be related by an impedance model, that is necessarily non-linear and depends on the fingertip specific characteristics (e.g., geometric parameters, subject's age). The use of a fingertip impedance model is necessary to solve the kinematics indeterminacy caused by the underactuation of our cutaneous system. In this work we assume a simplified fingertip impedance model, which is a linear relationship between the resultant wrench and the platform displacement. In other terms, we consider the platform configuration $\boldsymbol{\xi}$ proportional to the wrench $\mathbf{w_p}$,

$$\boldsymbol{\xi} = \mathbf{K}^{-1}\mathbf{w_p}, \tag{4}$$

where $\mathbf{K} \in \mathbb{R}^{6\times6}$ is the fingertip stiffness matrix, as defined in (Park et al. 2003).

Control. From the control point of view, the device can be represented as a non linear, multi-input multi-output (MIMO) coupled system. Moreover, the device is underactuated, since the number of actuators is lower than the degrees of freedom of the end-effector. It is therefore not possible to control at the same time both the platform position and the forces applied to the fingertip. In the two applications presented in this paper, we considered a force control approach, with the objective of regulating the forces applied at the fingertips. For a desired force $\mathbf{f_r}$, we estimate the corresponding target forces at the cables $\mathbf{t_{r,i}}$ by inverting the equilibrium relationship in eq. 2. As previously discussed, since the device is underactuated, this relationship cannot be directly inverted (i.e., there are wrenches $\mathbf{w_p}$ that cannot be balanced by the forces $\mathbf{t_{r,i}}$). In order to be able to solve the system in eq. 2, in our applications we disregarded the torque components $\mathbf{m}$. Before starting to use the device, the initial position of the mobile platform must be calibrated according to the size of the user's fingertip.

III. Peg-in-hole in a virtual environment

In order to evaluate the feasibility of the sensory subtraction approach in a complex scenario, we carried out two experiments. The first one consists of a peg-in-hole task in a virtual environment.

A. Experimental setup

Fig. 4 shows the experimental setup. The master system is composed of two cutaneous devices, attached to the end-effectors of two Omega.3 haptic interfaces, as also shown in Fig. 2b. The virtual environment is composed of a peg, a board with two holes (named $hole_1$ and $hole_2$ in Fig. 4b), and two small spheres.

The holes are 35 mm deep (x-direction), 35 mm wide (y-direction), and 5 mm high (z-direction). The peg is a 150 g cube with an edge length of 30 mm, and, therefore, the hole has a clearance of 5 mm in the x and y directions. The spheres have a diameter of 10 mm, and their position is linked to the virtual location of the subject's fingers, evaluated according to the popular god-object model (Zilles & Salisbury 1995) (i.e., the spheres are placed where the haptic interface end-effector would be if the haptic interface and the objects were infinitely stiff). A spring $k = 1$ N/mm is used to model the contact force between the spheres, controlled by the user, and the virtual objects. Subjects are able to interact with the virtual environment using CHAI 3D, an open-source set of C++ libraries for computer haptics and interactive real-time simulation.

B. Subjects

In order to determine the number of subjects needed for our research study, we ran a power analysis using the G*Power software. We estimated the effect size from the data retrieved in Pacchierotti et al. (2012a). Power analysis revealed that, in order to have a 95% chance of detecting differences among the metrics taken into account (completion time and exerted forces), we would need at least 15 participants (completion time: effect size 1.30, actual power 0.952; exerted forces: effect size 1.31, actual power 0.957).

Fifteen participants took part in the experiment, including ten males and five females. Seven of them had previous experience with haptic interfaces, but only three had tried cutaneous devices before. None of the participants reported any deficiencies in their visual or haptic perception abilities, and all of them were right-hand dominant. Participants were briefed about the task and afterward signed an informed consent, including the declaration of having no conflict of interest. All of them were able to give the consent autonomously. The participation in the experiment did not involve the processing of genetic information or personal data (e.g., health, sexual lifestyle, ethnicity, political opinion, religious or philosophical conviction), neither the tracking of the location or observation of the participants. Our organization does not require any IRB review for this case.

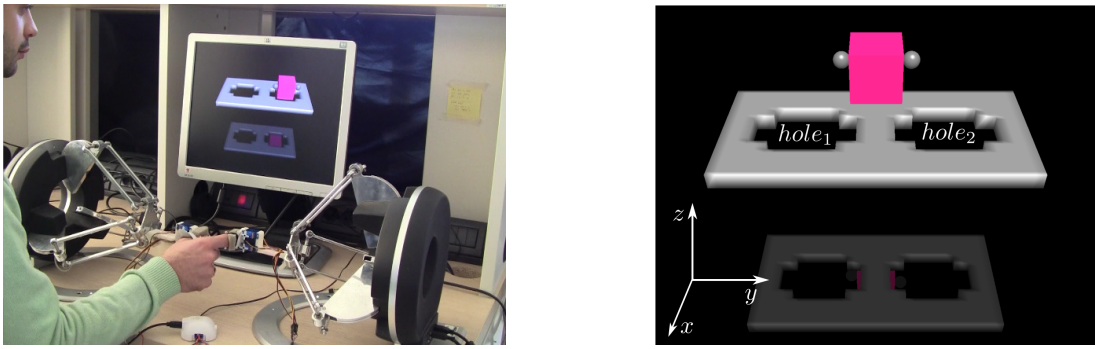

(a) Master system (b) Virtual environment

Fig. 4. Peg-in-hole in a virtual environment. Subjects are required to wear two cutaneous devices, one on the thumb and one on the index finger, and then complete the peg-in-hole task as fast as possible.

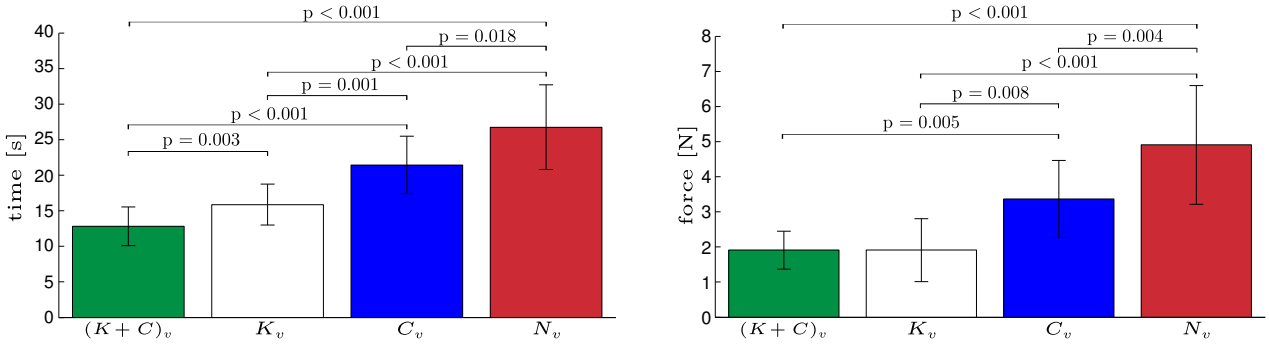

(a) Completion time (b) Contact force

Fig. 5. Peg-in-hole in a virtual environment. Completion time of the peg-in-hole task and force generated by the contact between the spheres and the object are plotted (mean and standard deviation) during tests with both kinesthetic and cutaneous force feedback (task $(K+C)_v$), kinesthetic only (task K_v), cutaneous only (task C_v), and no force feedback (task N_v). P-values of post-hoc group comparisons are reported when a statistical difference is present (confidence interval of 95%).

C. Methods

The task consisted of grasping the cube from the ground, inserting it into the right hole ($hole_2$), then in the left hole ($hole_1$), and then again in $hole_2$ and $hole_1$. The task started when the subject touched the object for the very first time and finished when the subject inserted, for the second time, the peg in $hole_1$. At least half of the length of the peg had to be inserted in each hole, from the top to the bottom. When the object was correctly inserted into the hole, the color of the peg changed[2]. In order to make the task easier to complete, the angular velocity of the peg was set to zero (i.e., the peg was not allowed to rotate).

After signing the informed consent, participants donned two cutaneous devices, one on the thumb and one on the index finger (see Fig. 4a), and were provided with a 10-minute familiarization period with the experimental setup. They were then asked to complete the peg-in-hole task as fast as possible.

Each participant made sixteen trials of the peg-in-hole task, with four randomized repetitions for each feedback condition proposed:

- kinesthetic and cutaneous feedback, provided by both the Omega and the cutaneous devices (full haptic feedback, condition $(K+C)_v$),
- kinesthetic feedback only, provided by the Omega interfaces (condition K_v),
- cutaneous feedback only, provided by the cutaneous devices (sensory subtraction approach, condition C_v),
- no haptic feedback (condition N_v).

In condition $(K+C)_v$, the force computed by the virtual environment is fed back by both the Omega interfaces and the cutaneous devices, assuming the two haptic stimuli to be provided independently from each other. In this case, in fact, each cutaneous device fastens to the corresponding finger with a strap between the PIP and DIP joints. For this reason we can assume the force provided by the Omega as applied only at that point. The cutaneous device is thus the only display providing cutaneous stimuli to the fingertip. Nonetheless, the Omega still provides cutaneous stimuli at the point where the strap is fastened, but we can consider this force negligible for our purposes.

In condition K_v, the cutaneous devices are not active: the force is provided by the Omega only, and the finger pulp is not in contact with the mobile platform. In this case we can consider the subject as receiving only kinesthetic feedback.

In condition C_v, the force is provided through the cutaneous devices only. In this case we can consider the subject as

[2]A video of the experiment in a virtual environment can be downloaded at http://goo.gl/jDfeJ5

Feedback condition	Completion time			Contact force		
	Statistic	df	Sig.	Statistic	df	Sig.
$(K+C)_v$	0.911	15	0.138	0.921	15	0.198
K_v	0.949	15	0.510	0.938	15	0.353
C_v	0.953	15	0.572	0.925	15	0.233
N_v	0.957	15	0.632	0.917	15	0.174

TABLE II
SHAPIRO-WILK NORMALITY TEST (VIRTUAL ENVIRONMENT).

receiving only cutaneous feedback. This is what Prattichizzo et al. (2012) called *sensory subtraction*, as it subtracts the kinesthetic part of the full haptic interaction to leave only cutaneous cues.

In condition N_v, no haptic feedback is provided to the subjects.

In all the conditions, the Omega interfaces are in charge of tracking the position of the fingers. Visual feedback is always provided to the subjects (see Fig. 4).

D. Results

In order to evaluate the performance of the considered feedback conditions, we recorded (1) the time needed to complete the task and (2) the forces generated by the contact between the two spheres, controlled by the subject, and the cube. Data resulting from different repetitions of the same condition, performed by the same subject, were averaged before comparison with other conditions' data. All the subjects were able to complete the task. In the following analysis, completion time and exerted forces are treated as dependent variables, while the feedback condition is treated as the independent variable.

Fig. 5a shows the average time elapsed between the instant the subject grasped the cube for the very first time and the instant he or she completed the peg-in-hole task. The collected data passed the Shapiro-Wilk normality test (see Table II for details) and the Mauchly's Test of Sphericity ($\chi^2(5) = 10.427$, $\mathrm{p} = 0.065$). Comparison of the means among the feedback condition was tested using a one-way repeated measures ANOVA ($F(3, 42) = 48.410$, $\mathrm{p} < 0.001$). The means differed significantly. Post-hoc analysis with Bonferroni adjustments revealed statistically significant difference between all the groups, showing that the time needed to complete the task depends on the feedback condition. Significant p-values of post-hoc group comparisons are reported in Fig. 5a (confidence interval of 95%).

Fig. 5b shows the average contact forces generated between the two spheres, controlled by the subject, and the cube along the y-direction, i.e., the one perpendicular to the cube surface (see Fig. 4b). The collected data passed the Shapiro-Wilk normality test (see again Table II). Mauchly's Test of Sphericity indicated that the assumption of sphericity had been violated ($\chi^2(5) = 16.988$, $p = 0.005$). A one-way repeated measures ANOVA with a Greenhouse-Geisser correction showed a statistically significant difference between the means of the four feedback conditions ($F(1.704, 23.861) = 27.046$, $\mathrm{p} < 0.001$). Post-hoc analysis with Bonferroni adjustments revealed no statistical significance between the two conditions employing kinesthetic feedback ($(K+C)_v$ and K_v), while it revealed a difference between the condition employing no force feedback (N_v) and the one using cutaneous feedback only (C_v). Moreover, there was a significant difference between condition C_v and conditions $(K+C)_v$ and K_v. Significant p-values of post-hoc group comparisons are reported in Fig. 5b (confidence interval of 95%).

Fig. 6 reports the position of the cube along the z- and y-axes. Average trajectory of the peg along the z- and y- axes (solid green line) $\pm$ standard deviation (green patch) along the z-axis is shown for each feedback condition. The size of the green patch gives a measure of the variability of the trajectory among the subjects.

E. Discussion

While receiving both kinesthetic and cutaneous feedback (condition $(K+C)_v$), subjects completed the task in less time than while receiving kinesthetic feedback only (condition K_v). Moreover, employing solely cutaneous feedback (sensory subtraction, condition C_v) yielded to significant better results than employing no force feedback at all (condition N_v), both in terms of completion time and exerted forces. A higher force fed back to the subjects meant a larger penetration into the virtual object and a higher energy expenditure during the grasp (Prattichizzo & Trinkle 2008).

Nonetheless, as expected, using kinesthetic feedback (both conditions $(K+C)_v$ and K_v) still showed better performance with respect to employing either cutaneous feedback only or no force feedback at all. However, we believe that this reduction of performance is a price worth paying in order to get a great improvement in the stability of the haptic loop, as it will be clear from the following experiment.

IV. PEG-IN-HOLE IN A REAL (TELEOPERATED) ENVIRONMENT

In the previous section, we analyzed the performance of cutaneous feedback with respect to full haptic feedback, kinesthetic feedback, and no force feedback at all. However, we did not evaluate how those conditions affect the overall stability of our control loop. In fact, time-varying destabilizing factors, such as hard contacts and communication delays, may significantly affect the stability of teleoperation systems with kinesthetic feedback, reducing their applicability and effectiveness (see Sec. I and Fig. 1a). On the other hand, we expect cutaneous feedback to not affect the stability of these systems, since the force is provided locally at the skin and does not influence the position of the master end-effector (see Sec. II-A and Fig. 1b).

Toward this objective, we carried out a second experiment that consists of a peg-in-hole task in a real (teleoperated) environment. In this experiment we only consider feedback conditions providing cutaneous cues. In fact, in terms of stability, we expect providing solely kinesthetic feedback to behave similarly to providing full haptic feedback (i.e., kinesthetic and cutaneous feedback). Likewise, we expect providing no force feedback at all to behave similarly to providing cutaneous feedback only.

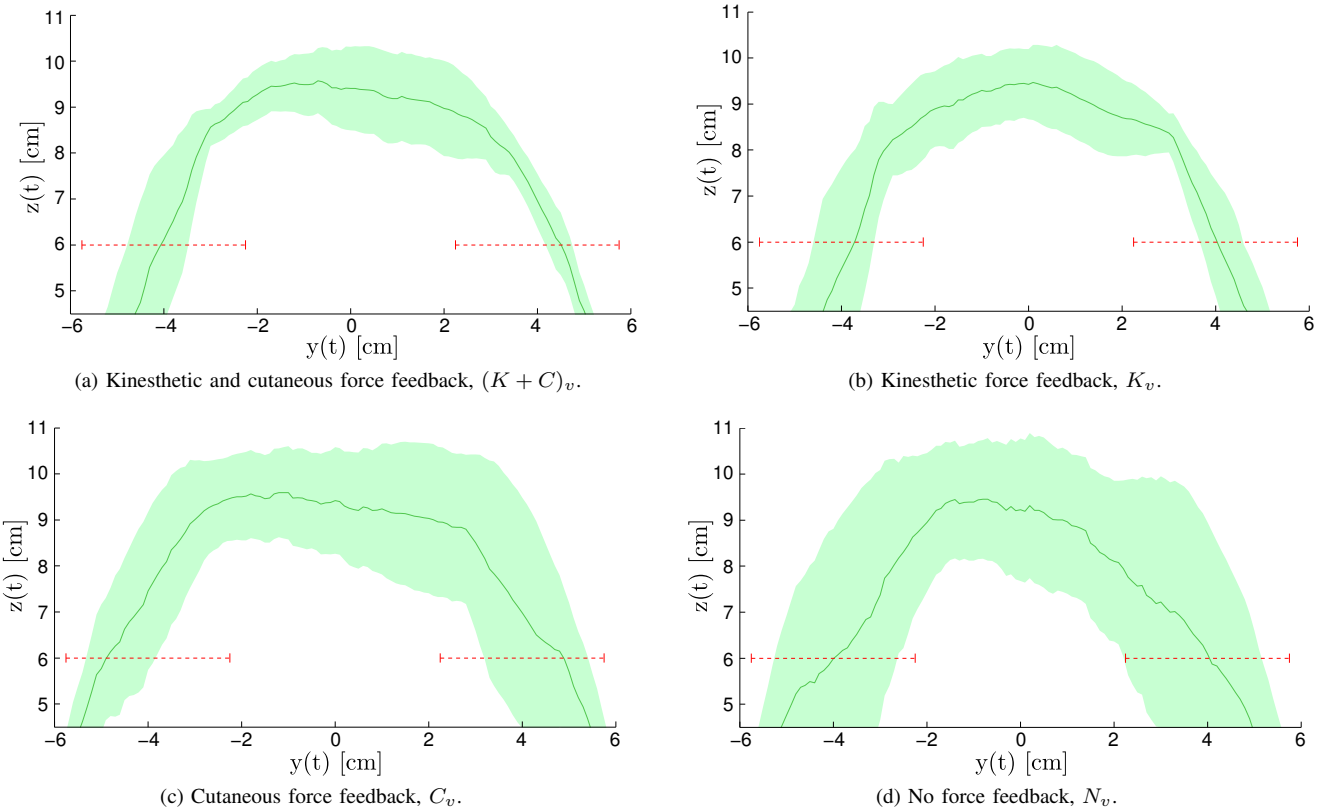

(a) Kinesthetic and cutaneous force feedback, $(K + C)_v$.

(b) Kinesthetic force feedback, K_v.

(c) Cutaneous force feedback, C_v.

(d) No force feedback, N_v.

Fig. 6. Peg-in-hole in a virtual environment. Average trajectory of the peg along the z- and y- axes (solid green line) $\pm$ standard deviation (green patch) along the z-axis is shown for each feedback condition. The position of the two holes (dashed red lines) are reported as well. Subjects were able to complete the peg-in-hole task in all the considered conditions. The size of the green patch gives a measure of the variability of the trajectory among the subjects.

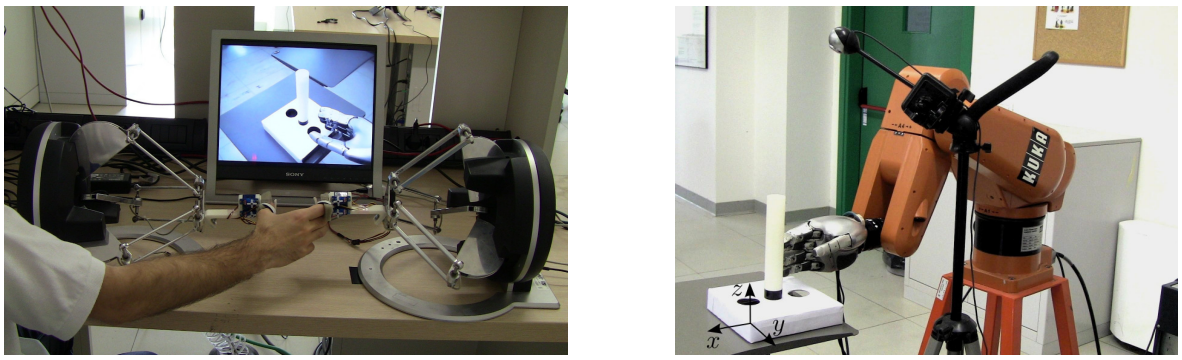

(a) Master system

(b) Slave system

Fig. 7. Peg-in-hole in a real (teleoperated) environment. The master side is composed of two cutaneous devices mounted on the end-effectors of two Omega.3 haptic devices, while the slave side consists of the DLR-HIT Hand II attached to the 6 DoFs manipulator KUKA KR3.

A. Experimental setup

Fig. 7 and 8 show the experimental setup. The master system again consists of two cutaneous devices attached to the end-effectors of two Omega.3 haptic interfaces. The slave system is composed of a 6 DoF manipulator KUKA KR3 and a DLR-HIT Hand II. The robotic hand is attached to the end-effector of the manipulator. A video camera is placed near the manipulator to let the operator see the hand and its nearby environment. The environment is composed of a cylinder of 150 g and a rigid board with two circular holes (see Fig. 7b). The holes have a diameter of 45 mm and are 35 mm high. The cylinder has a base radius of 35 mm and a height of 200 mm. Therefore, the hole has a radial clearance of 10 mm in the x-y plane. In this second experiment we used a cylinder so that peg's rotations about the z-axis did not prevent it from entering the holes, making the task easier to complete.

In order to ensure a convincing illusion of telepresence, the degrees of freedom of the operator's movements should be well replicated by the slave system (Massimino & Sheridan 1993). In our system the average position of the operator's fingers controls the telemanipulator wrist, and the distance between the two fingers is linked to the distance between the

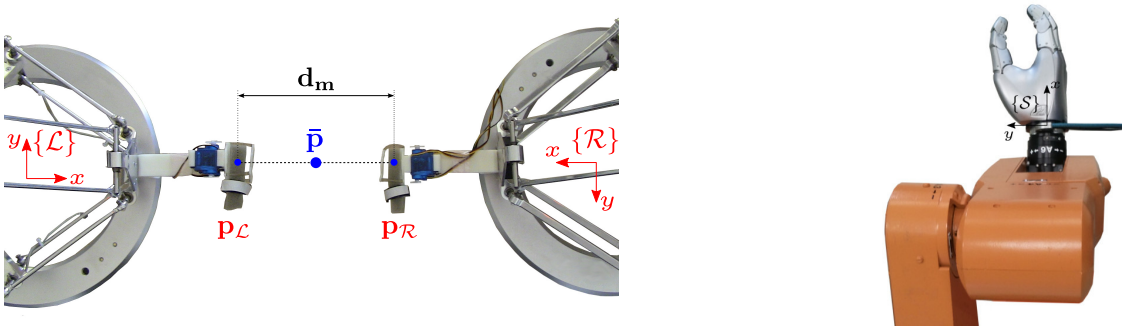

(a) Master system

(b) Slave system

Fig. 8. Peg-in-hole in a real (teleoperated) environment. $\{\mathcal{L}\}$ and $\{\mathcal{R}\}$ are two reference frames on the Omega haptic interfaces and $\bar{\mathbf{p}}$ is the point located between the two end effectors. Figure (b) shows the origin of the slave reference frame $\{\mathcal{S}\}$, that is placed on the robotic hand wrist.

thumb and index fingers of the robotic hand.

In Fig. 8a, let $\{\mathcal{L}\}$ and $\{\mathcal{R}\}$ be two reference frames, whose origins are located at the geometric center of the base of the left and right haptic interfaces, respectively. Points $\mathbf{p}_\mathcal{L}, \mathbf{p}_\mathcal{R} \in \mathbb{R}^3$ represent the positions of the haptic devices' end-effectors with respect to $\{\mathcal{L}\}$ and $\{\mathcal{R}\}$, respectively. Let $\mathbf{d} = [d_x \;\; d_y \;\; d_z]^T$ be the distance vector, expressed with respect to the $\{\mathcal{L}\}$ frame, between the origins of $\{\mathcal{L}\}$ and $\{\mathcal{R}\}$, $\mathbf{R_z}(\pi) \in \mathbb{R}^{3\times3}$ the π rotation matrix about the z-axis, and

$$\mathbf{H}_\mathcal{L}^\mathcal{R}(\pi, \mathbf{d}) = \begin{bmatrix} \mathbf{R_z}(\pi) & \mathbf{d} \\ \mathbf{0} & 1 \end{bmatrix} \tag{5}$$

the homogeneous transformation matrix from $\{\mathcal{R}\}$ to $\{\mathcal{L}\}$. Due to the relative positioning of the haptic interfaces and reference frames, only the first component of the distance vector, d_x, is different from zero. In order to keep the x axes of the two interfaces correctly aligned, the positioning of the haptic devices was carefully checked before the beginning of each experiment. The average position of the fingers can be then expressed as

$$\tilde{\bar{\mathbf{p}}} = \frac{1}{2}\left(\tilde{\mathbf{p}}_\mathcal{L} + \mathbf{H}_\mathcal{L}^\mathcal{R}(\pi, \mathbf{d})\, \tilde{\mathbf{p}}_\mathcal{R}\right), \tag{6}$$

with respect to $\{\mathcal{L}\}$, which is our base reference frame on the master side. From now on, we will consider the notation $\tilde{\mathbf{k}}$ to represent the vector $\mathbf{k} \in \mathbb{R}^3$ augmented by appending a "1", therefore $\tilde{\mathbf{k}} = [\mathbf{k}^T \quad 1]^T$.

Since the telemanipulator end-effector was controlled in velocity, the input command $\mathbf{v} \in \mathbb{R}^3$ can be expressed as

$$\mathbf{v} = \mathbf{R_z}\left(\frac{\pi}{2}\right)\, \dot{\bar{\mathbf{p}}}\,, \tag{7}$$

where $\dot{\bar{\mathbf{p}}} \in \mathbb{R}^3$ is the velocity of the midpoint $\bar{\mathbf{p}}$, located between the end effectors of the two Omega haptic interfaces, and $\mathbf{R_z}(\frac{\pi}{2}) \in \mathbb{R}^{3\times3}$ is the $\frac{\pi}{2}$ counter-clockwise rotation matrix about the z-axis, which performs the rotation from the master reference system $\{\mathcal{L}\}$ to the slave reference frame $\{\mathcal{S}\}$ (see Fig. 8b). For the sake of simplicity, and due to the nature of the telemanipulation task, the orientation of the robotic wrist was fixed.

For the robotic hand, the distance between the subject's fingers controlled the distance between the robotic ones. Let

$$\tilde{\mathbf{d}}_\mathbf{m} = \tilde{\mathbf{p}}_\mathcal{L} - \mathbf{H}_\mathcal{L}^\mathcal{R}(\pi, \mathbf{d})\, \tilde{\mathbf{p}}_\mathcal{R} \tag{8}$$

be the distance between the two master's end-effectors, expressed with respect to $\{\mathcal{L}\}$. Let us also define n_q as the number of joints of the robotic fingers and

$$\mathbf{d_s} = \mathbf{R_z}(\pi)\, \mathbf{d_m} \tag{9}$$

as the distance between the master's end-effectors with respect to $\{\mathcal{S}\}$. For the sake of simplicity, and due to the nature of the telemanipulation task, we actuated only movements along the y direction (with respect to $\{\mathcal{S}\}$). Changes in $\mathbf{d_s}$ controlled the velocity of the robotic thumb as

$$\dot{\mathbf{d}}_\mathbf{t} = \frac{\dot{\mathbf{d}}_\mathbf{s}}{2}, \tag{10}$$

and of the robotic index finger as

$$\dot{\mathbf{d}}_\mathbf{i} = \begin{pmatrix} 1 & 0 & 0 \\ 0 & -1 & 0 \\ 0 & 0 & 1 \end{pmatrix} \frac{\dot{\mathbf{d}}_\mathbf{s}}{2}\,. \tag{11}$$

The velocities of the robotic hand joints $\dot{q} \in \mathbb{R}^{2n_q}$ can thus be expressed as

$$\dot{\mathbf{q}} = \mathbf{J}^\# \dot{\mathbf{d}}_\mathbf{r}\, \zeta, \tag{12}$$

where $\mathbf{J}^\#$ is the Moore-Penrose pseudoinverse of the robotic hand Jacobian matrix $\mathbf{J} \in \mathbb{R}^{6\times2n_q}$, $\dot{\mathbf{d}}_\mathbf{r} = [\dot{\mathbf{d}}_\mathbf{t} \;\; \dot{\mathbf{d}}_\mathbf{i}]^\mathrm{T}$, and ζ is the scaling factor between the master and slave workspace. Due to the mechanical design of each robotic finger, that has only three joints, we assumed the robotic hand as not redundant, i.e., the null space $\mathcal{N}(\mathbf{J})$ is empty.

Similarly, contact forces $\boldsymbol{\lambda} \in \mathbb{R}^6$, exerted by the hand at the two contact points, can be expressed as

$$\boldsymbol{\lambda} = (\mathbf{J}^\mathrm{T})^\#\boldsymbol{\tau} + \mathbf{N}_{\mathbf{J}^\mathrm{T}}\, \boldsymbol{\chi}, \tag{13}$$

where $\mathbf{N}_{\mathbf{J}^\mathrm{T}}$ is a matrix whose columns form a basis of $\mathcal{N}(\mathbf{J}^\mathrm{T})$, and the vector $\boldsymbol{\chi}$ parametrizes the homogeneous solution to the equilibrium problem $\boldsymbol{\tau} = \mathbf{J}^\mathrm{T}\boldsymbol{\lambda}$. In the literature, generic contact forces that satisfy the condition $\mathbf{J}^\mathrm{T}\mathbf{N}_{\mathbf{J}^\mathrm{T}}\, \boldsymbol{\chi} = \mathbf{0}$ are referred as structural forces (Prattichizzo & Trinkle 2008).

Since we are interested in feeding back only forces due to the grasp, we filtered out the ones registered during free-hand movements.

The system is managed by a GNU/Linux machine, equipped with a real-time scheduler. It communicates via UDP/IP with the controller of the robotic hand and via Eth.RSIXML (KUKA Roboter GmbH, Germany) with the telemanipulator. The haptic and cutaneous devices use their own embedded microcontrollers and are connected to the GNU/Linux machine via USB. The master and slave systems are connected to the same Local Area Network (LAN). However, thanks to the underlying communication infrastructure, they could have been also easily placed in different LANs and then communicate through an Internet connection.

To preserve the stability of the teleoperation system, we employed the time-domain passivity controller presented by Franken et al. (2011). The control architecture is split into two separate layers. The hierarchical top layer, named *Transparency Layer*, aims at achieving the desired transparency, while the lower layer, named *Passivity Layer*, ensures the passivity of the system. Separate communication channels connect the layers at the slave and master levels so that information related to exchanged energy is separated from information about the desired behavior. However, the objective of this work is not the design of an efficient passivity controller, but the validation of the proposed cutaneous approach. We used a stability controller *only* to be able to compare full haptic feedback with our cutaneous-only sensory subtraction technique.

B. Subjects

The same fifteen participants who took part in the experiment of Sec. III participated in this one as well.

C. Methods

The task consisted of grasping the cylinder from its initial position (see Fig. 7b) and inserting it into two holes, following a sequence of insertion analogous to the one already described in Sec. III-D. The task started when the subject touched the object for the first time and finished when the subject inserted, for the second time, the peg in the hole closer to the manipulator. At least half of the length of the peg had to be inserted in the hole, from the top to the bottom. The grasp had to be performed using the fingertip of the robotic hand[3].

Participants donned two cutaneous devices, one on the thumb and one on the index finger (see Fig. 7a), and were provided with a 10-minute familiarization period with the experimental setup. They were then asked to complete the peg-in-hole task as fast as possible.

Each participant made twelve trials of the peg-in-hole task, with four randomized repetitions for each force feedback condition proposed:

- kinesthetic and cutaneous feedback, provided by the Omega and the cutaneous devices, employing the passivity controller described at the end of Sec. IV-A (full haptic feedback, condition $(K+C+P)_r$),
- kinesthetic and cutaneous feedback, provided by the Omega and the cutaneous devices (full haptic feedback, no stability controller, condition $(K+C)_r$),
- cutaneous feedback only, provided by the cutaneous devices (sensory subtraction approach, condition C_r).

In condition $(K+C+P)_r$, the contact force $\boldsymbol{\lambda}$ registered at the robotic fingers (see eq. 13), is fed back by both the Omega interfaces and the cutaneous devices. The passivity controller guarantees the stability of the system. This represents our ideal condition, when the subject is provided with full haptic feedback and no unstable behavior arise.

Condition $(K+C)_r$ is similar to condition $(K+C+P)_r$. The contact force $\boldsymbol{\lambda}$ is again fed back by both the Omega interfaces and the cutaneous devices. However, this time, no passivity algorithm guarantees the stability of the teleoperation loop.

In condition C_r, the contact force $\boldsymbol{\lambda}$ is provided through the cutaneous devices only. This is our cutaneous-only sensory subtraction condition.

In all the conditions, the Omega interfaces are in charge of tracking the position of the fingers. Visual feedback, as shown in Fig. 7a, is always provided to the subjects by a video camera placed next to the manipulator arm.

D. Results

In order to evaluate the performance of the different feedback conditions, we recorded (1) the task success rate, (2) the time needed to complete the task, and (3) the forces generated by the contact between the two spheres, controlled by the subject, and the cylinder. Data resulting from different repetitions of the same condition, performed by the same subject, were averaged before comparison with other conditions' data. In the following analysis, success rate, completion time, and exerted forces are treated as dependent variables, while the feedback condition is treated as the independent variable.

Fig. 9a shows the average task success rate. A trial was considered *not* successful if the subject was not able to complete the peg-in-hole task (i.e., the peg fell out of the workspace of the slave robot). Success rates for conditions $(K+C+P)_r$, $(K+C)_r$, and C_r were 100%, $(23.3\pm19.97)\%$, and 100%, respectively. The main reason for failing the task during condition $(K+C)_r$ was the presence of large oscillations, due to the lack of any stability control technique (see Extension 3). No time limit was imposed.

For the completion time and the average exerted forces, we analyzed only conditions $(K+C+P)_r$ and C_r, since condition $(K+C)_r$ was clearly unsuitable due to its unstable behavior. Fig. 9b shows the average time elapsed between the instant the subject touches the object for the first time and the instant he or she completes the peg-in-hole task. The collected data passed Shapiro-Wilk normality test (see Table III for details). A paired-samples t-test determined that the time needed to complete the task differed statistically significantly between

[3]A video of the experiment in a real environment can be downloaded at http://goo.gl/Xs9nUs

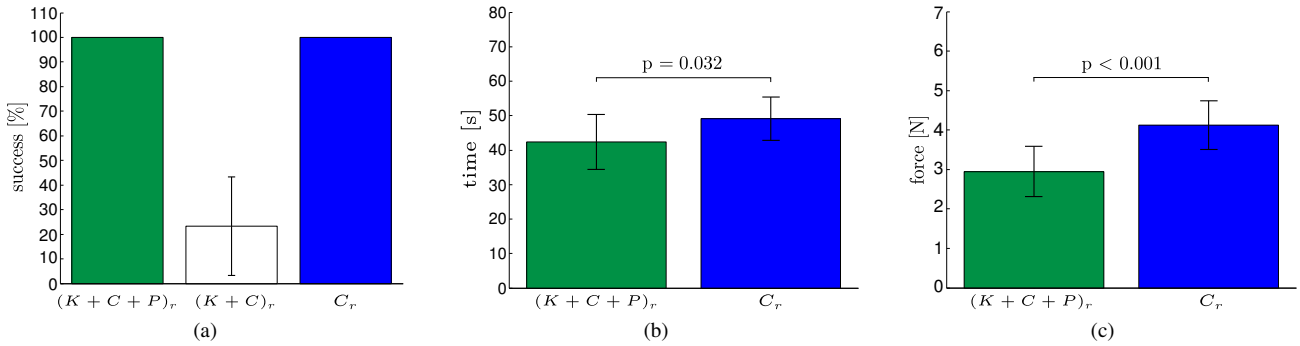

Fig. 9. Peg-in-hole in a real (teleoperated) environment. (a) Average task success rate during tests with both kinesthetic and cutaneous feedback (conditions $(K+C+P)_r$ and $(K+C)_r$), and cutaneous feedback only (condition C_r) is plotted (mean and standard deviation). (b) Completion time of the peg-in-hole task and (c) force generated by the contact between the two robotic fingers and the object, with kinesthetic and cutaneous feedback (condition $(K+C+P)_r$), and cutaneous feedback only (condition C_r) are plotted (mean and standard deviation). P-values of paired t-tests are reported in (b) and (c) when a statistical difference is present (confidence interval of 95%).

Feedback condition	Completion time			Contact force		
	Statistic	df	Sig.	Statistic	df	Sig.
$(K+C+P)_r$	0.937	15	0.351	0.940	15	0.383
C_r	0.963	15	0.744	0.960	15	0.687

TABLE III
SHAPIRO-WILK NORMALITY TEST (REAL ENVIRONMENT).

feedback conditions ($(K+C+P)_r$ vs. C_r, $t(14) = -2.381$, $p = 0.032$, confidence interval of 95%).

Fig. 9c shows the average forces generated by the contact between the two robotic fingers, controlled by the subject, and the peg along the y-direction of $\{\mathcal{S}\}$ (see Fig. 8b). The collected data passed Shapiro-Wilk normality test (see again Table III). A paired-samples t-test determined that the average force exerted differed statistically significantly between feedback conditions ($(K+C+P)_r$ vs. C_r, $t(14) = -5.594$, $p < 0.001$, confidence interval of 95%).

Fig. 10 reports the average trajectory of the peg during the task. Trajectories were averaged among subjects for each feedback condition. Average trajectory of the peg along the z- and y- axes (solid blue line) $\pm$ standard deviation (blue patch) along the z-axis is shown for each feedback condition. The size of the blue patch gives a measure of the variability of the trajectory among the subjects.

E. Discussion

In this second experiment we extended the evaluation of our cutaneous-only sensory subtraction approach to a real scenario. Subjects were required to complete a teleoperated peg-in-hole task in three different feedback conditions. Comparing success rates during conditions $(K+C)_r$ and C_r shows the improvement in *stability* of our cutaneous-only approach (see also Extension 3). On the other hand, comparing completion times and exerted forces during conditions $(K+C+P)_r$ and C_r let us quantitatively analyze the loss of *performance* due to the absence of the kinesthetic component of the haptic interaction.

The intrinsic stability of cutaneous feedback has been already discussed in Sec. I, assessed in (Pacchierotti et al. 2012a, Prattichizzo et al. 2012, Pacchierotti et al. 2014, 2012b), and here again highlighted by the success rates of the feedback conditions: 23% for $(K+C)_r$ versus 100% for C_r. As it also clear from Extension 3, the oscillations arose during condition $(K+C)_r$ made it very difficult for the subjects to complete the peg-in-hole task. On the other hand, employing cutaneous feedback alone (sensory subtraction) made the system stable, even without enforcing a stability control technique. Since the force is applied directly to the fingertips and does not affect the position of the end-effector of the master device, it is straightforward to assess that sensory subtraction would make *any* teleoperation system intrinsically stable (see Fig. 1b). However, it is also obvious that employing kinesthetic feedback in a stiff environment, without any stability control strategy, brings the system near to instability, making the trials difficult to complete. Nonetheless, in order to emphasize the stability properties of our approach, we decided to include condition $(K+C)_r$ anyway.

The price for this improvement in stability is a significant loss of performance. In fact, in condition $(K+C+P)_r$ subjects completed the task in less time and exerted less force with respect to condition C_r. This means that full haptic feedback (if no oscillations arise) still leads to better performance with respect to employing cutaneous feedback alone.

These results are in agreement with previous findings in the literature. Pacchierotti et al. (2012b), for example, analyzed the performance of sensory subtraction for a needle insertion task in a real scenario. They employed a 1-DoF cutaneous device to remotely teleoperate a needle mounted on a robotic manipulator. Cutaneous feedback made the subjects able to successfully complete the task, it outperformed visual substitution of force and also made the system intrinsically stable. However, as expected, kinesthetic feedback (when no oscillations arose) showed better performance. Meli et al. (2014) found the same type of cutaneous feedback more effective than sensory substitution via either visual or auditory feedback in a pick-and-place task similar to the da Vinci Skills Simulator's Pegboard task. King et al. (2009a) presented a pneumatic cutaneous feedback system for robotic surgery and evaluated it in a peg transfer tasks with 20 subjects

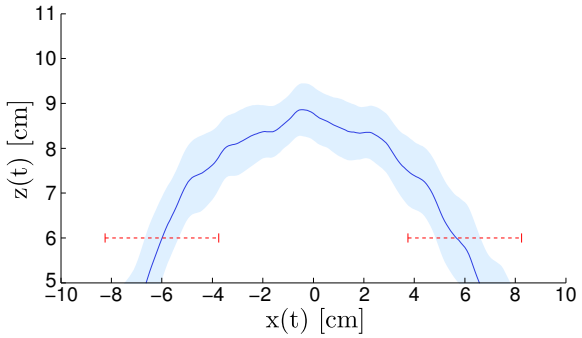

(a) Kinesthetic and cutaneous force feedback, employing the passivity controller, $(K+C+P)_r$.

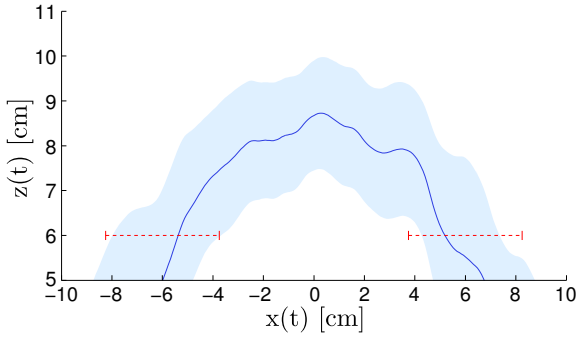

(b) Kinesthetic and cutaneous force feedback, no passivity controller, $(K+C)_r$.

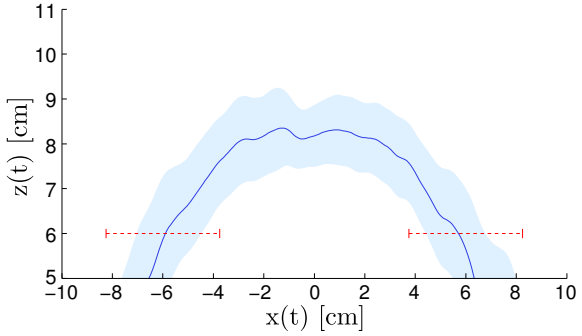

(c) Cutaneous force feedback, C_r.

Fig. 10. Peg-in-hole in a real (teleoperated) environment. Average trajectory of the peg along the z- and x- axes (solid blue line) $\pm$ standard deviation (blue patch) along the z-axis is shown for each feedback condition. The position of the two holes (dashed red lines) are reported as well. The size of the blue patch gives a measure of the variability of the trajectory among the subjects.

(including 4 surgeons). All subjects used lower force when the cutaneous feedback system was active. McMahan et al. (2011) developed a cutaneous system for the Intuitive da Vinci robot that enables a surgeon to feel instrument vibrations in real time. 114 surgeons and non-surgeons tested this system in dry-lab manipulation tasks and expressed a significant preference for the inclusion of cutaneous feedback (Koehn & Kuchenbecker 2014). van Der Putten et al. (2010) presented a cylindrical rotating device able to provide slip sensations to the fingertip. In order to understand the influence of skin stretch and tangential motion feedback on laparoscopic grasp control, the authors carried out a two-handed lifting experiment employing two custom laparoscopic graspers. Subjects who received cutaneous feedback could control their pinch force significantly better than subjects who did not receive cutaneous feedback. More recently, Prattichizzo et al. (2013) carried out a curvature discrimination experiment and found out that employing a cutaneous device together with a popular haptic interface improved the performance with respect to employing the haptic interface alone. Similarly, Frisoli et al. (2008) found a higher curvature discrimination threshold value for kinesthetic feedback alone with respect to providing both cutaneous and kinesthetic cues.

V. Conclusions and Future Work

In this work we analyze the feasibility, effectiveness, and implications of providing solely cutaneous feedback in robotic teleoperation. Prattichizzo et al. (2012) call this feedback approach *sensory subtraction*, as it subtracts the destabilizing kinesthetic part of the full haptic interaction to leave only cutaneous cues. For this purpose, we developed a 3-DoF cutaneous display. It is composed of a static body that houses three servo motors above the user's fingernail and a mobile platform that applies the requested stimuli to the fingertip. In comparison to similar existing cutaneous devices, the one presented here has three actuated degrees of freedom, high peak force and accuracy, and it is able to provide the sensation of breaking and making contact with virtual and remote surfaces. Moreover, it can be easily attached to the end-effector of existing grounded haptic interfaces. We carried out two peg-in-hole experiments, both in a virtual environment and in a real (teleoperated) environment. Results demonstrated the feasibility of employing sensory subtraction in robotic teleoperation. Cutaneous feedback showed better performance than employing no force feedback at all, but, as expected, it was outperformed by full haptic feedback provided by grounded haptic interfaces. However, the proposed cutaneous-only approach guaranteed the intrinsic stability of the teleoperation system and kept the system stable even in the absence of a stability controller. In the same condition, full haptic feedback showed highly degraded performance. In applications where the safety of the system is a paramount and non-negotiable feature (e.g., robotic surgery), this loss of performance may be a price worth paying to get a great improvement in the stability of the teleoperation loop.

Work is in progress to design new cutaneous displays with better dynamic performance, higher accuracy, and direct measurement of the force applied to the fingertip. Stereographic vision will be employed to provide better depth perception, and the video camera will be placed closer to the natural body-centric view, in order to provide a more natural point of view on the environment. Finally, we will test our cutaneous-only approach in a medical scenario, where the safety guaranteed by our technique is a valuable feature. We also plan to compare our approach with other common sensory substitution techniques (e.g., vibrotactile, audio and visual feedback) and evaluate user's experience through a bipolar Likert-type questionnaire.

Acknowledgment

The research leading to these results has received funding from the European Union Seventh Framework Programme

FP7/2007-2013 under grant agreement n°601165 of the project "WEARHAP - WEARable HAPtics for humans and robots" and from the Italian Ministry of Education, Universities and Research Futuro in Ricerca 2012 Programme under grant agreement RBFR12C608 of the project "MODELACT".

REFERENCES

Birznieks, I., Jenmalm, P., Goodwin, A. W., & Johansson, R. S. (2001). 'Encoding of direction of fingertip forces by human tactile afferents'. *The Journal of Neuroscience* **21**(20):8222–8237.

Edin, B. B. & Johansson, N. (1995). 'Skin strain patterns provide kinaesthetic information to the human central nervous system.'. *The Journal of physiology* **487**(1):243–251.

Franken, M., Stramigioli, S., Misra, S., Secchi, C., & Macchelli, A. (2011). 'Bilateral telemanipulation With time delays: a two-layer approach combining passivity and transparency'. *IEEE Transactions on Robotics* **27**(4):741–756.

Frisoli, A., Solazzi, M., Salsedo, F., & Bergamasco, M. (2008). 'A fingertip haptic display for improving curvature discrimination'. *Presence: Teleoperators and Virtual Environments* **17**(6):550–561.

Hannaford, B. (1987). 'Task-level testing of the JPL-OMV smart end effector'. In *Proceedings of the Workshop on Space Telerobotics*, vol. 2.

Hayward, V., Astley, O. R., Cruz-Hernandez, M., Grant, D., & Robles-De-La-Torre, G. (2004). 'Haptic interfaces and devices'. *Sensor Review* **24**(1):16–29.

Hirche, S., Ferre, M., Barrio, J., Melchiorri, C., & Buss, M. (2007). 'Bilateral control architectures for telerobotics'. In *Advances in Telerobotics*, pp. 163–176. Springer.

Hokayem, P. & Spong, M. (2006). 'Bilateral teleoperation: An historical survey'. *Automatica* **42**(12):2035–2057.

Johnson, K. O. (2001). 'The roles and functions of cutaneous mechanoreceptors'. *Current opinion in neurobiology* **11**(4):455–461.

Kim, J. & Ryu, J. (2010). 'Robustly stable haptic interaction control using an energy-bounding algorithm'. *The International Journal of Robotics Research* **29**(6):666–679.

King, C.-H., Culjat, M. O., Franco, M. L., Bisley, J. W., Carman, G. P., Dutson, E. P., & Grundfest, W. S. (2009a). 'A multielement tactile feedback system for robot-assisted minimally invasive surgery'. *IEEE Transactions on Haptics* **2**(1):0052–56.

King, C.-H., Culjat, M. O., Franco, M. L., Lewis, C. E., Dutson, E. P., Grundfest, W. S., & Bisley, J. W. (2009b). 'Tactile feedback induces reduced grasping force in robot-assisted surgery'. *IEEE Transactions on Haptics* **2**(2):103–110.

Kitagawa, M., Dokko, D., Okamura, A. M., & Yuh, D. D. (2005). 'Effect of sensory substitution on suture-manipulation forces for robotic surgical systems'. *Journal of Thoracic and Cardiovascular Surgery* **129**(1):151–158.

Koehn, J. K. & Kuchenbecker, K. J. (2014). 'Surgeons and non-surgeons prefer haptic feedback of instrument vibrations during robotic surgery'.

Kontarinis, D. A. & Howe, R. D. (1995). 'Tactile display of vibratory information in teleoperation and virtual environments'. *Presence: Teleoperators and Virtual Environments* **4**(4):387–402.

Kurita, Y., Yonezawa, S., Ikeda, A., & Ogasawara, T. (2011). 'Weight and friction display device by controlling the slip condition of a fingertip'. In *Proc. IEEE/RSJ International Conference on Intelligent Robots and Systems (IROS)*, pp. 2127–2132.

Lawrence, D. A. (1993). 'Stability and transparency in bilateral teleoperation'. *IEEE Transactions on Robotics and Automation* **9**(5):624–637.

Lee, D. & Huang, K. (2010). 'Passive-set-position-modulation framework for interactive robotic systems'. *IEEE Transactions on Robotics* **26**(2):354–369.

Li, M., Luo, S., Seneviratne, L., Nanayakkara, T., Althoefer, K., & Dasgupta, P. (2013). 'Haptics for Multi-fingered Palpation'. In *Proc. IEEE International Conference on Systems, Man, and Cybernetics*, pp. 4184–4189.

Massimino, M. J. (1995). 'Improved force perception through sensory substitution'. *Control Engineering Practice* **3**(2):215–222.

Massimino, M. J. & Sheridan, T. B. (1993). 'Sensory substitution for force feedback in teleoperation'. *Presence: Teleoperators and Virtual Environments* **2**(4):344–352.

Massimino, M. J. & Sheridan, T. B. (1994). 'Teleoperator performance with varying force and visual feedback'. *Human Factors: The Journal of the Human Factors and Ergonomics Society* **36**(1):145–157.

McMahan, W., Gewirtz, J., Standish, D., Martin, P., Kunkel, J. A., Lilavois, M., Wedmid, A., Lee, D. I., & Kuchenbecker, K. J. (2011). 'Tool contact acceleration feedback for telerobotic surgery'. *IEEE Transactions on Haptics* **4**(3):210–220.

Meli, L., Pacchierotti, C., & Prattichizzo, D. (2014). 'Sensory subtraction in robot-assisted surgery: fingertip skin deformation feedback to ensure safety and improve transparency in bimanual haptic interaction.'. *IEEE Transactions on Biomedical Engineering* **61**(4):1318–1327.

Moody, L., Baber, C., & Arvanitis, T. N. (2002). 'Objective surgical performance evaluation based on haptic feedback'. *Studies in health technology and informatics* **85**:304–310.

Niemeyer, G. & Slotine, J. J. E. (2004). 'Telemanipulation with time delays'. *The International Journal of Robotics Research* **23**(9):873–890.

Pacchierotti, C., Chinello, F., Malvezzi, M., Meli, L., & Prattichizzo, D. (2012a). 'Two Finger Grasping Simulation with Cutaneous and Kinesthetic Force Feedback'. *Haptics: Perception, Devices, Mobility, and Communication* pp. 373–382.

Pacchierotti, C., Chinello, F., & Prattichizzo, D. (2012b). 'Cutaneous device for teleoperated needle insertion'. In *Proceedings of the IEEE RAS & EMBS International Conference on Biomedical Robotics and Biomechatronics*, pp. 32–37.

Pacchierotti, C., Prattichizzo, D., & Kuchenbecker, K. J. (2015). 'Cutaneous feedback of fingertip deformation and vibration for palpation in robotic surgery'. *IEEE Transactions on Biomedical Engineering. In Press* .

Pacchierotti, C., Tirmizi, A., & Prattichizzo, D. (2014). 'Im-

proving transparency in teleoperation by means of cutaneous tactile force feedback'. *ACM Transactions on Applied Perception* **11**(1):4.

Park, K. H., Kim, B. H., & Hirai, S. (2003). 'Development of a soft-fingertip and its modeling based on force distribution'. In *Proceedings of the IEEE International Conference on Robotics and Automation*, vol. 3, pp. 3169–3174.

Prattichizzo, D., Chinello, F., Pacchierotti, C., & Malvezzi, M. (2013). 'Towards wearability in fingertip haptics: a 3-DoF wearable device for cutaneous force feedback'. *IEEE Transactions on Haptics* **6**(4):506 – 516.

Prattichizzo, D., Pacchierotti, C., Cenci, S., Minamizawa, K., & Rosati, G. (2010). 'Using a fingertip tactile device to substitute kinesthetic feedback in haptic interaction'. *Haptics: Generating and Perceiving Tangible Sensations* pp. 125–130.

Prattichizzo, D., Pacchierotti, C., & Rosati, G. (2012). 'Cutaneous Force Feedback as a Sensory Subtraction Technique in Haptics'. *IEEE Transactions on Haptics* **5**(4):289–300.

Prattichizzo, D. & Trinkle, J. (2008). *Chapter 28 on "Grasping". Handbook of Robotics*. Springer.

Provancher, W. R. & Sylvester, N. D. (2009). 'Fingerpad skin stretch increases the perception of virtual friction'. *IEEE Transactions on Haptics* **2**(4):212–223.

Quek, Z. F., Schorr, S., Nisky, I., Provancher, W., & Okamura, A. M. (2015). 'Sensory Substitution and Augmentation using 3-Degree-of-Freedom Skin Deformation Feedback'. *IEEE Transactions on Haptics* In Press.

Quek, Z. F., Schorr, S. B., Nisky, I., Okamura, A. M., & Provancher, W. R. (2013). 'Sensory Augmentation of Stiffness using Fingerpad Skin Stretch'. In *Proceedings of the IEEE World Haptics Conference*, pp. 467–472.

Ryu, J., Kwon, D., & Hannaford, B. (2004). 'Stable teleoperation with time-domain passivity control'. *IEEE Transactions on Robotics and Automation* **20**(2):365–373.

Salcudean, S. (1998). 'Control for teleoperation and haptic interfaces'. *Control problems in robotics and automation* pp. 51–66.

Salisbury, K. & Tarr, C. (1997). 'Haptic rendering of surfaces defined by implicit functions'. In *ASME Dynamic Systems and Control Division*, vol. 61, pp. 61–67.

Schoonmaker, R. E. & Cao, C. G. L. (2006). 'Vibrotactile force feedback system for minimally invasive surgical procedures'. In *Proceedings of the IEEE International Conference on Systems, Man and Cybernetics*, vol. 3, pp. 2464–2469.

Sheridan, T. B. (1989). 'Telerobotics'. *Automatica* **25**(4):487–507.

Sheridan, T. B. (1992). *Telerobotics, automation, and human supervisory control*. The MIT press.

Sheridan, T. B. (1995). 'Teleoperation, telerobotics and telepresence: A progress report'. *Control Engineering Practice* **3**(2):205–214.

Solazzi, M., Provancher, W. R., Frisoli, A., & Bergamasco, M. (2011). 'Design of a SMA actuated 2-DoF tactile device for displaying tangential skin displacement'. In *Proceedings of the IEEE World Haptics Conference*, pp. 31–36.

van Der Putten, E. P. W., Van den Dobbelsteen, J. J., Goossens, R. H., Jakimowicz, J. J., & Dankelman, J. (2010). 'The effect of augmented feedback on grasp force in laparoscopic grasp control'. *IEEE Transactions on Haptics* **3**(4):280–291.

van der Schaft, A. (2000). *L2-gain and passivity techniques in nonlinear control*.

Wagner, C. R., Stylopoulos, N., & Howe, R. D. (2002). 'The role of force feedback in surgery: analysis of blunt dissection'. In *Proceedings of the 10th Symposium of Haptic Interfaces for Virtual Environment and Teleoperator Systems*, pp. 68–74.

Webster III, R. J., Murphy, T. E., Verner, L. N., & Okamura, A. M. (2005). 'A novel two-dimensional tactile slip display: design, kinematics and perceptual experiments'. vol. 2, pp. 150–165.

Wiertlewski, M. & Hayward, V. (2012). 'Mechanical behavior of the fingertip in the range of frequencies and displacements relevant to touch'. *Journal of Biomechanics* **45**(11):1869 – 1874.

Zilles, C. B. & Salisbury, J. K. (1995). 'A constraint-based god-object method for haptic display'. In *Proceedings of the IEEE International Conference on Human Robot Interaction and Cooperative Robots*, vol. 3, pp. 146–151.